iScience

CellPress

Article

Charge Characteristics of Agouti-Related Protein Implicate Potent Involvement of Heparan Sulfate Proteoglycans in Metabolic Function

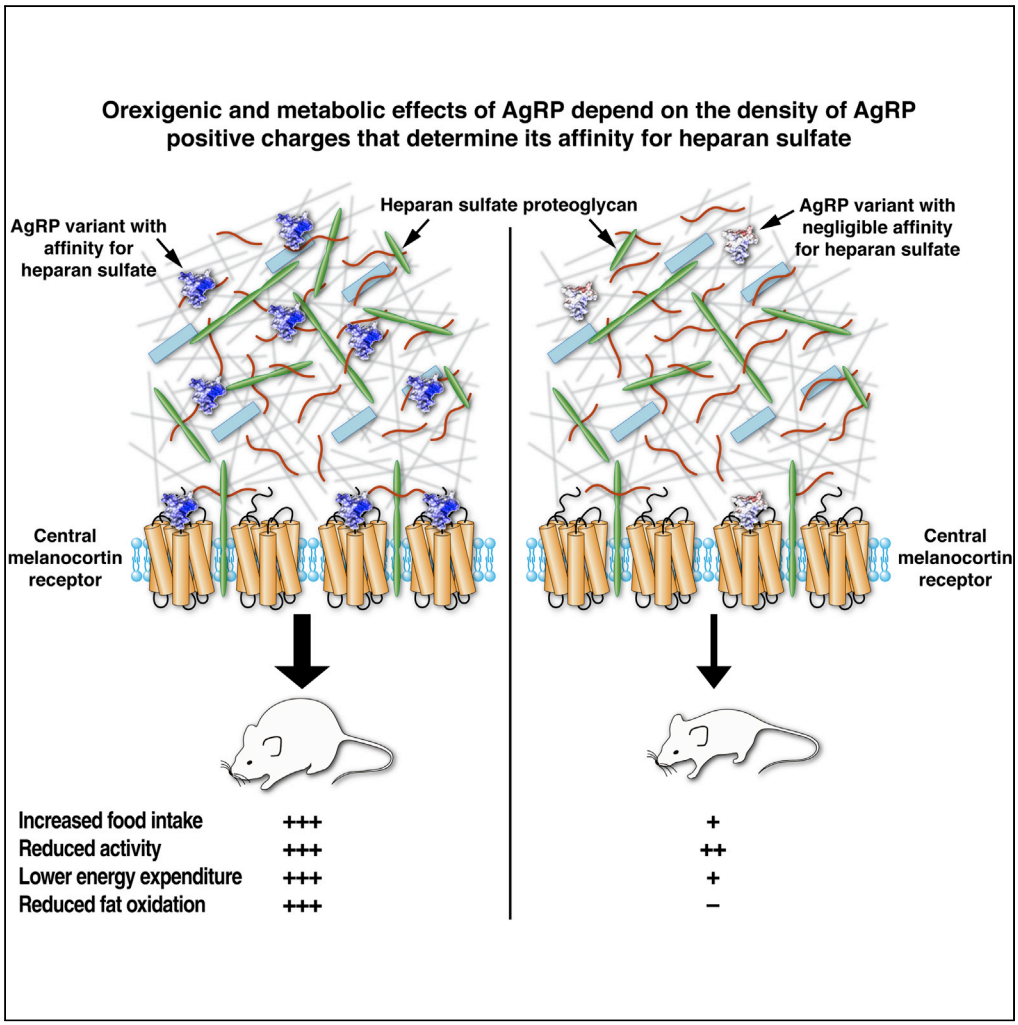

Jihuan Chen, Valerie Chen, Tomoya Kawamura, ..., Vez Repunte-Canonigo, Glenn L. Millhauser, Pietro Paolo Sanna

glennm@ucsc.edu (G.L.M.)
psanna@scripps.edu (P.P.S.)

HIGHLIGHTS

AgRP increases both *ad libitum* and operant food intake and reduces energy expenditure

AgRP reduces fat utilization as a fuel source, which promotes body fat accumulation

These actions of AgRP depend on the positive charges, outside its ICK motif, that bind heparan sulfate

Chen et al., iScience *22*, 557–570
December 20, 2019 © 2019 The Authors.
https://doi.org/10.1016/j.isci.2019.10.061

iScience

CellPress

Article

Charge Characteristics of Agouti-Related Protein Implicate Potent Involvement of Heparan Sulfate Proteoglycans in Metabolic Function

Jihuan Chen,[1,5] Valerie Chen,[2,5] Tomoya Kawamura,[1] Ivy Hoang,[1] Yang Yang,[1] Ashley Tess Wong,[2] Ryan McBride,[3,4] Vez Repunte-Canonigo,[1] Glenn L. Millhauser,[2,*] and Pietro Paolo Sanna[1,6,*]

SUMMARY

The endogenous melanocortin peptide agouti-related protein (AgRP) plays a well-known role in foraging, but its contribution to metabolic regulation is less understood. Mature $AgRP_{(83-132)}$ has distinct residues for melanocortin receptor binding and heparan sulfate interactions. Here, we show that AgRP increases *ad libitum* feeding and operant responding for food in mice, decreases oxygen consumption, and lowers body temperature and activity, indicating lower energy expenditure. AgRP increased the respiratory exchange ratio, indicating a reduction of fat oxidation and a shift toward carbohydrates as the primary fuel source. The duration and intensity of AgRP's effects depended on the density of its positively charged amino acids, suggesting that its orexigenic and metabolic effects depend on its affinity for heparan sulfate. These findings may have major clinical implications by unveiling the critical involvement of interactions between AgRP and heparan sulfate to the central regulation of energy expenditure, fat utilization, and possibly their contribution to metabolic disease.

INTRODUCTION

There is a pressing need to identify the underlying mechanisms of metabolic disease. The central melanocortin system regulates feeding, body weight, and energy expenditure. However, the contribution of the central melanocortin peptide agouti-related protein (AgRP) and its interaction with heparan sulfate to metabolic regulation has not been characterized. Here, we found that AgRP increases both *ad libitum* food intake and motivation for food in an operant paradigm and reduces energy expenditure and fat oxidation, which has been linked to a higher risk for metabolic disease. Both orexigenic and metabolic actions of AgRP depended on the density of AgRP positive charges, which determines its affinity for heparan sulfate independently of the binding of AgRP to central melanocortin receptors. These results support a role for heparan sulfate in the regulation of energy homeostasis by the melanocortin system.

The central melanocortin system includes neurons in the arcuate nucleus (ARC) of the hypothalamus that coexpress agouti-related protein (AgRP) and neuropeptide Y (NPY) and the neurotransmitter γ-aminobutyric acid (GABA) and neurons that coexpress proopiomelanocortin (POMC) and cocaine- and amphetamine-regulated transcript (CART; van der Klaauw, 2018). Evidence from mutant mice and human mutations indicates that the central melanocortin system plays a key role in coordinating nutrient intake, energy metabolism, fat accumulation, and body weight (Butler et al., 2000; Chen et al., 2000; Ehtesham et al., 2019; Lede et al., 2016; Nuutinen et al., 2018). However, the contribution of AgRP to metabolic regulation is not well understood because of its coexpression with GABA (Krashes et al., 2013) and NPY, which is also a key regulator of appetite and energy balance (Loh et al., 2015).

Neuropeptide Y/AgRP-coexpressing neurons promote feeding and weight gain, whereas POMC neurons attenuate feeding and promote weight loss (Dodd and Tiganis, 2017). Both NPY/AgRP and POMC/CART neurons express receptors for the adipocyte-derived hormone leptin and insulin that, together with other hormones (e.g., the gut peptides ghrelin and peptide YY, among others) and nutrients, such as glucose, fatty acids, and peptides, allow them to sense peripheral energy status and needs (van der Klaauw, 2018). Circulating leptin and insulin interact with neurons in the ARC through special properties of the blood-brain barrier in this region of the hypothalamus, resulting in the inhibition of NPY/AgRP neurons and activation of POMC/CART neurons, leading to a reduction of food intake (Dodd and Tiganis, 2017).

[1]Department of Immunology, The Scripps Research Institute, La Jolla, CA 92037, USA

[2]Department of Chemistry and Biochemistry, University of California, Santa Cruz, CA 95064, USA

[3]Department of Molecular Medicine, The Scripps Research Institute, La Jolla, CA 92037, USA

[4]Genomics Core, The Scripps Research Institute, La Jolla, CA 92037, USA

[5]These authors contributed equally

[6]Lead Contact

*Correspondence: glennm@ucsc.edu (G.L.M.), psanna@scripps.edu (P.P.S.)

https://doi.org/10.1016/j.isci.2019.10.061

This is an open access article under the CC BY-NC-ND license (http://creativecommons.org/licenses/by-nc-nd/4.0/).

Numerous studies support a central role for NPY/AgRP neurons in regulating energy expenditure, food intake, and body weight. NPY/AgRP neurons mediate insulin's central effects on hepatic glucose production (Konner et al., 2007; Obici et al., 2002; Pocai et al., 2005). Fat accumulation and obesity comprise the primary phenotype of lower central melanocortin-3 receptor (MC3R) and MC4R loss-of-function (Butler et al., 2000; Chen et al., 2000; Ehtesham et al., 2019; Lede et al., 2016; Nuutinen et al., 2018). Insulin receptor signaling in NPY/AgRP neurons in the ARC inhibits hepatic glucose production via vagus nerves that are associated with food intake (Konner et al., 2007; Obici et al., 2002; Pocai et al., 2005). Additionally, NPY/AgRP neurons control insulin sensitivity by regulating brown adipose tissue (BAT; Steculorum et al., 2016). The deletion of suppressor of cytokine signaling 3 (SOCS3) in NPY/AgRP or POMC/CART neurons enhanced insulin signaling and improved whole-body glucose metabolism in diet-induced obese mice (Dodd and Tiganis, 2017). The deletion of activating transcription factor 4 (ATF4) in NPY/AgRP neurons resulted in a lean phenotype with an increase in energy expenditure and resistance to high fat diet (HFD)-induced obesity (Deng et al., 2017).

The melanocortin system includes five G protein-coupled receptors (GPCRs) that contribute to diverse physiological processes (Goodfellow and Saunders, 2003; Kalra et al., 1999; Williams et al., 2001). Agonists of MCRs derive from POMC through proteolytic cleavage to produce adrenocorticotropic hormone (ACTH) and various melanocyte-stimulating hormone (MSH) variants, such as α-MSH, β-MSH, and γ-MSH. MC1R is involved in skin and hair pigmentation by regulating the production of melanin (Goodfellow and Saunders, 2003; Kalra et al., 1999; Williams et al., 2001). MC2R is mainly expressed in the adrenal cortex where it serves as an ACTH receptor, inducing glucocorticoid production (Schioth et al., 1996). MC3Rs and MC4Rs are expressed in the brain and involved in the regulation of energy homeostasis and metabolism (Goodfellow and Saunders, 2003; Kalra et al., 1999; Williams et al., 2001). α-MSH is released by POMC/CART neurons and acts as the endogenous agonist of central MC3Rs and MC4Rs. Central MC4Rs and peripheral MC1Rs exhibit elevated basal activity in the absence of agonists, and their activity is regulated by two pivotal endogenous peptides that act as inverse agonists: AgRP in the central nervous system (CNS) and agouti-signaling protein (ASP; the main product of the agouti gene in the skin; Goodfellow and Saunders, 2003; Kalra et al., 1999; Williams et al., 2001).

AgRP is a key modulator of central MC3Rs and MC4Rs (Cone et al., 2001). Full-length AgRP is a 132-residue pro-protein that is posttranslationally processed by pro-protein convertase 1/3 into its mature form, $AgRP_{(83-132)}$ (Creemers et al., 2006). $AgRP_{(83-132)}$ contains five disulfide bonds, three of which form an inhibitor cystine knot (ICK) motif (Figure 1), which is sufficient for MC3/4R antagonism (McNulty et al., 2001), whereas positively charged residues in the N-terminal segment and C-terminal loop allow AgRP to bind heparan sulfate (Palomino et al., 2017) independently of its receptor affinity and signaling ability through a reduction of cyclic adenosine monophosphate (cAMP; Madonna et al., 2012).

Heparan sulfate proteoglycans were originally considered structural elements of the extracellular matrix, but they have subsequently emerged as key modulators of biological processes (Kim et al., 2011; Sarrazin et al., 2011). Sulfate groups provide docking sites for numerous positively charged peptide ligands, including AgRP, that are involved in diverse biological processes (Kim et al., 2011; Sarrazin et al., 2011).

The contribution of AgRP and its interaction with heparan sulfate to metabolic regulation has not been previously characterized. The present study investigated the effects of AgRP peptides, including $AgRP_{(83-132)}$ (i.e., the mature form of AgRP) and two charge-modified AgRP variants that differed in their affinity for heparan sulfate, on food intake and energy metabolism. We found that the intracerebroventricular (ICV) administration of AgRP in addition to *ad libitum* feeding in the home cage increased operant responding for food in a manner that depended on the density of AgRP positive charges, which determined its affinity for heparan sulfate. Similarly, we found that AgRP decreased energy expenditure and shifted fuel utilization from fatty acids toward carbohydrates, which also required heparan sulfate binding. Lower fatty acid oxidation at rest promotes an increase in fat storage (Must et al., 1999) and is associated with a higher risk of type 2 diabetes and metabolic syndrome (Rosenkilde et al., 2010; Ukropcova et al., 2007). All of the AgRP variants reduced body temperature and activity, suggesting lower energy expenditure. However, the effects of the variant that had a lower density of positive charges had faster onsets and were less protracted.

Overall, the present results indicate that the orexigenic effects of AgRP are accompanied by complex metabolic changes that are characterized by lower energy expenditure, a reduction of fat oxidation, and a shift in substrate utilization toward carbohydrate oxidation. Although the AgRP variants that were tested

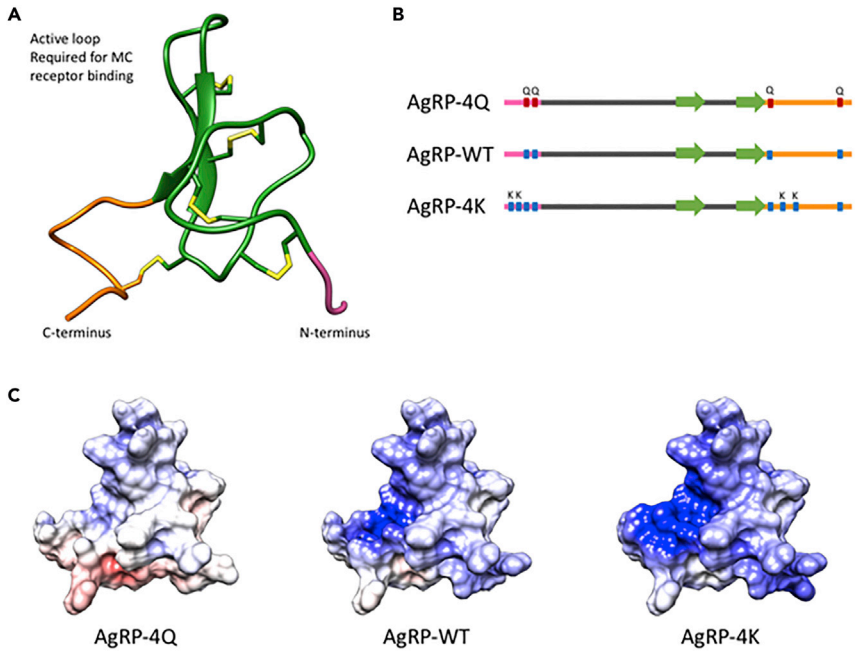

Figure 1. Structure and Electrostatic Potential Maps for AgRP and Charge-Modified AgRP Variants

(A) Nuclear magnetic resonance structure (Protein DataBank: 1HYK) of mature AgRP-WT$_{(83\text{-}132)}$ depicting the inhibitor cystine knot (ICK) core (green) and non-ICK N-terminal segment (pink) and C-terminal loop (orange). Disulfide-bonds are in yellow. The ICK core that contains the active loop is sufficient for MC3/4R binding and antagonism. However, the N-terminal segment and C-terminal loop that flank the ICK core are highly conserved and required for AgRP-induced long-term feeding.

(B) Schematic diagram of the location of lysine mutations in AgRP-4K and glutamine mutations in AgRP-4Q. All charge mutations are located outside of the ICK core.

(C) Electrostatic potential surface maps for AgRP-4Q, AgRP-WT, and AgRP-4K, calculated by Adaptive Poisson-Boltzmann Solver (APBS). AgRP-4K adds positive charges to an existing positively charged patch that is present in AgRP-WT.

did not differ in receptor affinity or *in vitro* potency, their *in vivo* potency and duration of action significantly depended on positively charged amino acids that mediate heparan sulfate binding.

METHODS

Peptide Synthesis, Purification, and Folding

The AgRP peptide sequences were previously described in Madonna et al., 2012. The peptide was produced on a CEM Liberty1 microwave peptide synthesizer using standard Fmoc (fluorenylmethyloxycarbonyl chloride) chemistry. Amino acids were purchased from AAPPTec and assembled on H-Rink amide ChemMatrix resin. Fmoc protecting groups were removed using 20% piperidine and 0.1 M hydroxybenzotriazole (HOBt) in dimethylformamide (DMF). Each amino acid was double coupled using four molar equivalents of Fmoc-amino acid, five molar equivalents of diisopropylcarbodiimide (DIC), and 10 molar equivalents of HOBt in DMF. Cleavage of the peptide from resin was performed in a trifluoroacetic acid (TFA)/triisopropylsilane (TIS)/1,2-ethanedithiol (EDT)/phenol (90:4:4:2) mixture for 90 min. The resin was filtered, and the filtrate was added to 90 mL of cold dry diethyl ether. The precipitate was collected by centrifugation, and the diethyl ether was discarded. Oxidative folding was achieved in folding buffer (2.0 M GuHCl/0.1 M Tris, 3 mM GSH, 400 μM GSSG [pH 8–8.5]) at a peptide concentration of 0.1 mg/mL and stirred for 24 h. Folding was monitored by reverse-phase HPLC, which revealed one major species that was used in subsequent experiments. The folded products were purified on a C18 reverse-phase HPLC column and identified as fully oxidized peptides and confirmed with the correct molecular weight by electrospray ionization-mass spectrometry.

Glycan Array Fabrication

Amine(-NH_2)-linked heparan sulfate glycan compounds (Glycan Therapeutics) were immobilized on NHS-activated surface-coated slides (Nexterion Slide-H, Applied Microarrays) using a robotic microarray printer

(Microgrid II, Digilab) that was equipped with StealthSMP4B microarray pins (Telechem) to couple heparan sulfate glycan compounds by covalent binding via (-NH_2) reactive chemistry. Custom printing was performed by the robotic pin deposition of 0.6 nL of (-NH_2)-conjugated heparan sulfate glycan compounds in print buffer (150 mM phosphate [pH 8.5], which contained 0.01% Tween 20) onto Nexterion-Slide H glass slides (Applied Microarrays). Slide printing with the heparan sulfate glycan compounds was kept at 80% relative humidity for 1 h, followed by desiccation overnight. Printed slide microarrays were placed in a sealed slide box and stored at −20°C. Before use, unreacted NHS groups on the printed slides were immersed in blocking buffer (50 mM ethanolamine in 50 mM borate buffer [pH 9.2]) for 1 h. The slides were then rinsed with water and dried before the binding assays.

Heparan Sulfate-AgRP Binding Assay

The printed slides were pre-wetted with Tris-Metal-Salts (TMS) buffer (25 mM Tris, 2.7 mM KCl, 2 mM $CaCl_2$, 2 mM $MgCl_2$, and 137 mM NaCl [pH 7.4], containing 0.05% Triton X-100). Peptides of $AgRP_{(83-132)}$ and AgRP charge variants were then diluted to 50 μg/mL in TMS buffer and directly applied to the pre-wetted arrays. After incubation at room temperature for 1 h, the AgRP solution or its variants were removed, and the arrays were washed with TMS buffer three successive times. A pre-complexed antibody mixture of Rb anti-human AgRP (10 μg/mL, Novus Biologicals) and anti-Rb IgG-Alexa 488 (5 μg/mL, Life Technologies) was subsequently added to the arrays and incubated for an additional 1 h at room temperature. The slides were washed by successive rinses with TMS, TMS without Triton X-100, and deionized H_2O. The washed arrays were dried by centrifugation and immediately scanned for green fluorescence using an InnoScan confocal microarray scanner (Innopsys, Carbonne, France). Images were analyzed using Mapix software and processed with ImageJ software.

Animals

Male C57BL/6 mice, 20–24 weeks old, were single-housed in a climate-controlled vivarium on a 12 h/12 h light/dark cycle (lights on 6:00 AM to 6:00 PM) and fed a standard diet (58 kcal% carbohydrate, 17 kcal% fat, and 25 kcal% protein; LM-485; Teklad Diets, Madison, WI, USA). Daily food consumption was measured by weighing the pellets in the home cage every day at the same time while the mice's body weights were recorded. All of the procedures adhered to the National Institutes of Health Guide for the Care and Use of Laboratory Animals (eighth edition) and were approved by the Institutional Animal Care and Use Committee of The Scripps Research Institute.

Ad Libitum Food Intake and Operant Responding for Food

Daily *ad libitum* food consumption was measured manually by weighing the standard laboratory chow (Teklad LM-485, catalog no. 7012, Teklad Diets, Madison, WI, USA) that was placed in the home cage. Body weights at the corresponding times were also monitored daily. For operant responding for food, the mice were trained to lever-press for food pellets in operant chambers (Med Associates, St. Albans, VT, USA) as described previously with minor modifications. For three days before training, 20 food pellets (14 mg, Bio-Serv, 64.5 kcal% carbohydrate, 10.1 kcal% fat, and 25.4 kcal% protein; total energy, 3.35 kcal/g) were placed in the home cage to prevent potential effects of neophobia on operant performance. The mice were trained 1 h/day under a fixed-ratio 1 (FR1) schedule, in which each active lever-press resulted in the delivery of one pellet, accompanied by illumination of the cue light above the lever that signaled a 5-s time-out period. Water was available from a sipper in the front side of the wall opposite the levers and food receptacle. After the mice developed stable responding for food ($\geq$20 rewards received per session and $\geq$75% total responses at the active lever over three consecutive sessions), the response requirement was gradually increased from FR1 to FR5 until stable responding was reached for two consecutive sessions.

Comprehensive Lab Animal Monitoring System

The comprehensive lab animal monitoring system (CLAMS; Columbus Instruments) is an open-circuit indirect calorimeter that allows simultaneous multiple parameter scoring, including measurements of gas concentrations and flow, core body temperature, activity, feeding, drinking, etc. Oxygen consumption (VO_2) is a measure of the volume of oxygen that is used to convert energy substrate into adenosine triphosphate. Energy expenditure can thus be assessed by measuring core body temperature and VO_2. The mice were acclimated to the CLAMS chambers for 72 h before they received an injection of AgRP and then were recorded for five days after the injection. Food and water were provided in the chamber *ad libitum* throughout the experiments. The RER (i.e., the ratio of VO_2 to CO_2 production) can be used to estimate the fuel source. An RER = 0.7 indicates that

fatty acids are the predominant fuel source for oxidative metabolism. An RER = 0.85 suggests a mix of fat and carbohydrates. An RER ≥1.00 indicates that carbohydrates are the primary fuel source (Lusk, 1924; Marvyn et al., 2016; Schmidt-Nielsen, 1997; Speakman, 2013).

Intracranial Cannula Implantation and ICV Microinjection Procedure

Intracranial stereotaxic surgery was performed as described previously (Chen et al., 2013). Briefly, the mice were immobilized in a stereotaxic frame in the flat-skull position (Kopf Instruments), and a cannula (26 gauge, Plastics One, Roanoke, VA, USA) was implanted in the lateral ventricle (anterior/posterior, −0.22 mm; medial/lateral, 1.0 mm; dorsal/ventral, −1.5 mm). The mice were allowed to recover from surgery for 7–10 days. On the test day, a stainless-steel injector (33 gauge, extended 1 mm below the tip of the cannula; Plastics One, Roanoke, VA, USA) was inserted into the cannula, and the AgRP solution (1 nmole in 1 μL of saline) was delivered slowly at a rate of 0.5 μL/min through the injector by a syringe pump (KD Scientific). The injector remained in place for 2 min to allow for diffusion and then was withdrawn slowly to avoid backflow of the fluid.

Data Analysis

Two-way repeated-measures analysis of variance (ANOVA) was used to assess the main effects of AgRP treatment. Significant differences between the AgRP group and vehicle control group were assessed using Fisher's Least Significant Difference *post hoc* test. Values of $p < 0.05$ were considered statistically significant. All of the behavioral data are expressed as means ± SEM and were analyzed using GraphPad Prism 8.0 software.

RESULTS

Binding of AgRP and Charge-Modified AgRP Variants to Heparan Sulfate Glycan Arrays

As shown in Figure 2, the mature form of AgRP ($AgRP_{[83-132]}$), henceforth referred to as wild-type AgRP (AgRP-WT), binds broadly to different heparan-sulfate-derived oligosaccharides in glycan arrays. AgRP binding affinity was correlated with the state of sulfation and length of the heparan sulfate oligosaccharides. AgRP binding appeared to be favored by 6S and NS sulfation but not by 3S sulfation. We next compared the binding of AgRP-WT and two charge-modified AgRP variants, including AgRP-4Q (in which positive charges were eliminated by replacing Arg and Lys residues with Gln) and AgRP-4K (in which additional positively charged amino acids were included by mutating Gly123 and Ala125 and the two Ser residues in the N-terminal segment to Lys; Madonna et al., 2012). These modifications have been shown to not affect MC3R or MC4R binding (Madonna et al., 2012). As shown in Figure 3, these two charge-modified AgRP variants resulted in alterations of the affinity for heparan sulfate in a glycan array using immobilized hexasaccharide that was representative of a highly sulfated heparan sulfate. AgRP-4Q exhibited negligible binding to sulfated hexasaccharide, whereas AgRP-4K exhibited approximately 50-times greater binding than AgRP-WT (Figure 3).

Effects of Charge-Modified AgRP Variants on *ad libitum* Food Intake and Body Weight

We first tested the effects of AgRP-WT and AgRP variants with a decrease or an increase in positive charges (AgRP-4Q and AgRP-4K, respectively) on *ad libitum* food intake in mice in their home cages (Figure 4). Each AgRP variant was injected ICV into the lateral ventricle. Food consumption and body weight were measured daily. As shown in Figure 4, the ICV administration of AgRP-WT and AgRP-4K but not AgRP-4Q significantly increased food intake and body weight. AgRP-4K exerted a more pronounced and long-lasting effect than AgRP-WT.

Effects of Charge-Modified AgRP Variants on Operant Responding for Food

We then tested the effects of AgRP variants in an operant food self-administration paradigm. The mice were trained in an operant chamber to obtain food pellets by pressing a lever on the wall. During the training phase, an FR1 schedule was used, whereby one active lever press resulted in the delivery of one food pellet. After the acquisition of stable lever-pressing behavior, the mice were gradually switched to an FR5 schedule and then remained at this FR throughout the remainder of the experimental period. AgRP-4Q, the variant with a decrease in positive charges, significantly and rapidly increased food responding on the first day of the injection, but the effect subsided within a few hours (Figure 5A). AgRP-4K, the variant with an increase in positive charges, induced a delayed increase in responding for food, starting approximately 10 h after the injection. However, the AgRP-4K-induced increase in responding for food

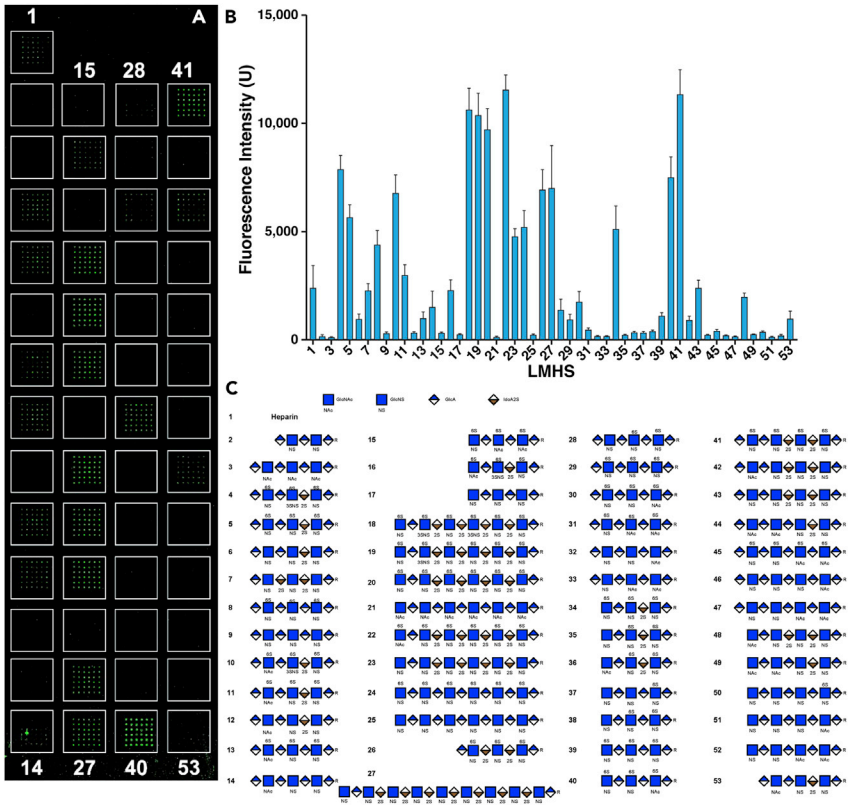

Figure 2. Glycan Array Analysis of AgRP Binding to Heparan Sulfate Oligosaccharides

(A) Fluorescent image of the glass slide glycan arrays showing fluorescence signals (green dots) of AgRP binding to 52 immobilized heparan sulfate oligosaccharides (low-molecular-weight heparan sulfate, LMHS).

(B) Bar graph showing the relative fluorescence intensity of AgRP binding to the heparan sulfate oligosaccharides arrays. Heparan sulfate oligosaccharides 22 and 41 show the highest intensity.

(C) The structures of the different heparan sulfate oligosaccharides on the slide microarray in A. Data are represented as mean ± SEM.

was quite protracted and statistically significant for five days (Figure 5B). Altogether, these results indicated that the positive charge and affinity of AgRP for heparan sulfate were associated with an increase in food intake and motivation for food.

Effects of Charge-Modified AgRP Variants on Energy Expenditure and Fuel Source

We next investigated the effects of AgRP variants on energy expenditure and fuel source using CLAMS chambers. One hour before being placed in the CLAMS chamber, the mice received an injection of AgRP-WT, AgRP-4Q, or AgRP-4K. Body temperature, VO_2, and carbon dioxide production (VCO_2) were recorded continuously for five days. The respiratory exchange ratio (RER; i.e., the ratio of VCO_2 to VO_2) was calculated to estimate the fuel source that was utilized for energy production, based on the difference in the number of oxygen molecules that are required for the oxidation of glucose *vs.* fatty acids.

All three AgRP variants reduced body temperature, suggesting a decrease in energy expenditure (Figure 6A). The reductions of body temperature that were induced by AgRP-WT and AgRP-4K had later onsets and were more protracted than the reduction that was induced by AgRP-4Q (Figure 6A). AgRP-WT also significantly reduced VO_2 for a protracted time (Figure 6B, left). AgRP-4K, but not AgRP-4Q, showed a similar protracted trend toward a VO_2 reduction, but this reduction did not reach statistical significance (Figure 6B, right).

AgRP-WT and AgRP-4K, but not AgRP-4Q, significantly increased the RER at rest (during the light, inactive phase), indicating a reduction of fat oxidation and a shift in fuel utilization toward carbohydrates at rest (Figure 6C). AgRP-4K also caused a significant short-term elevation of VCO_2 (not shown). Collectively, these

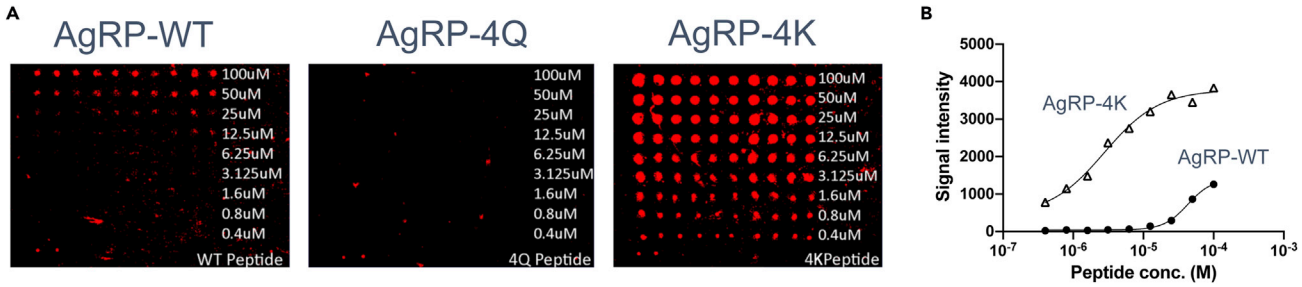

Figure 3. Binding of AgRP and Charge-Modified AgRP Variants to a Heparan Sulfate Hexasaccharide Glycan Array

(A) $AgRP_{(83-132)}$ (AgRP-WT) and AgRP-4K, in which Gly123 and Ala125 and the two Ser residues in the N-terminal segment were replaced with Lys, showed concentration-dependent binding to a glycan array of the heparan sulfate hexasaccharide GlcNS6S-GlcA-GlcNS6S-IdoA2S-GlcNS6S-GlcA-NH_2 (Array 34 in Figure 2 is the hexasaccharide used in this figure). The printed concentration of hexasaccharides was from 100 μM and serially diluted by a dilution factor of 2 down to a minimum concentration of 0.4 μM. Each concentration had 10 replicates. AgRP-4Q, in which Arg and Lys residues were replaced with Gln, showed negligible binding to the heparan sulfate hexasaccharide glycan array.

(B) Semiquantitative determination of binding of AgRP variants to heparan sulfate hexasaccharide glycan array. The signal intensity (arbitrary units) was determined by ImageJ software. The AgRP-4K binding curve showed a dramatic leftward shift that was indicative of approximately 50-times greater binding affinity for the heparan sulfate hexasaccharide glycan array than AgRP-WT. Data are represented as mean ± SEM.

results indicate that AgRP decreases energy expenditure, reduces fat oxidation, and increases carbohydrate oxidation. AgRP-WT significantly decreased energy expenditure, measured by VO_2.

All three AgRP variants reduced body temperature, regardless of their positive charges. However, reductions of body temperature that were induced by AgRP-WT and AgRP-4K (i.e., the more positively charged AgRP variants with affinity for heparan sulfate) had a more delayed onset, were more protracted, and were associated with a decrease in fat oxidation and an increase in carbohydrate oxidation.

Effects of Charge-Modified AgRP Variants on Activity, Feeding, and Drinking in CLAMS Chambers

Activity was assessed by the triple-axis detection of animal motion using the infrared photocell technology of the CLAMS. All three variants of AgRP significantly decreased total activity, ambulation, and rearing during the dark cycle (Figure 7). The AgRP-4Q-induced reduction of activity had a faster onset and a shorter duration than the AgRP variants that had greater positive charges, suggesting that heparan sulfate binding contributes to the duration of the AgRP-induced downregulation of activity. Access to food and water can be simultaneously monitored automatically in the CLAMS. AgRP-WT and AgRP-4K but not AgRP-4Q significantly increased both food and water intake (Figures 8 and 9). These results indicate that the AgRP variants decreased activity, regardless of their positive charges. However, the reductions of activity that were induced by the more positively charged AgRP variants (AgRP-WT and AgRP-4K) had a more delayed onset, were more protracted, and were associated with increases in food and water intake.

DISCUSSION

Neurons in the ARC of the hypothalamus that express the peptides AgRP and NPY and the neurotransmitter GABA promote feeding and weight gain and repress energy expenditure, whereas neurons that express POMC and CART inhibit food intake (Dodd and Tiganis, 2017). The specific contributions of these peptides and their classic neurotransmitter systems to feeding have only recently begun to be elucidated (Andermann and Lowell, 2017), but their respective functions in metabolic control are less characterized.

Interactions between AgRP and its central receptors are believed to be facilitated by heparan sulfate proteoglycan binding (Reizes et al., 2001), which has been proposed to act as a co-receptor and storage mechanism for heparan sulfate binding peptides such as AgRP (Kim et al., 2011; Sarrazin et al., 2011). Consistent with this view, the genetic ablation of heparanase, which selectively cleaves heparan sulfate chains, increases fat mass (Karlsson-Lindahl et al., 2012). Conversely, heparanase-overexpressing transgenic mice have lower body fat, despite an increase in food intake, and exhibit a greater utilization of fat as the main fuel source (Karlsson-Lindahl et al., 2012). The activation of NPY/AgRP neurons in the ARC by designer receptor exclusively activated by designer drugs (DREADDs) technology or optogenetics increases both *ad libitum* food intake and the motivation to work for food reinforcement in mice (Aponte et al., 2011; Krashes et al., 2011). However, AgRP neurons were found not

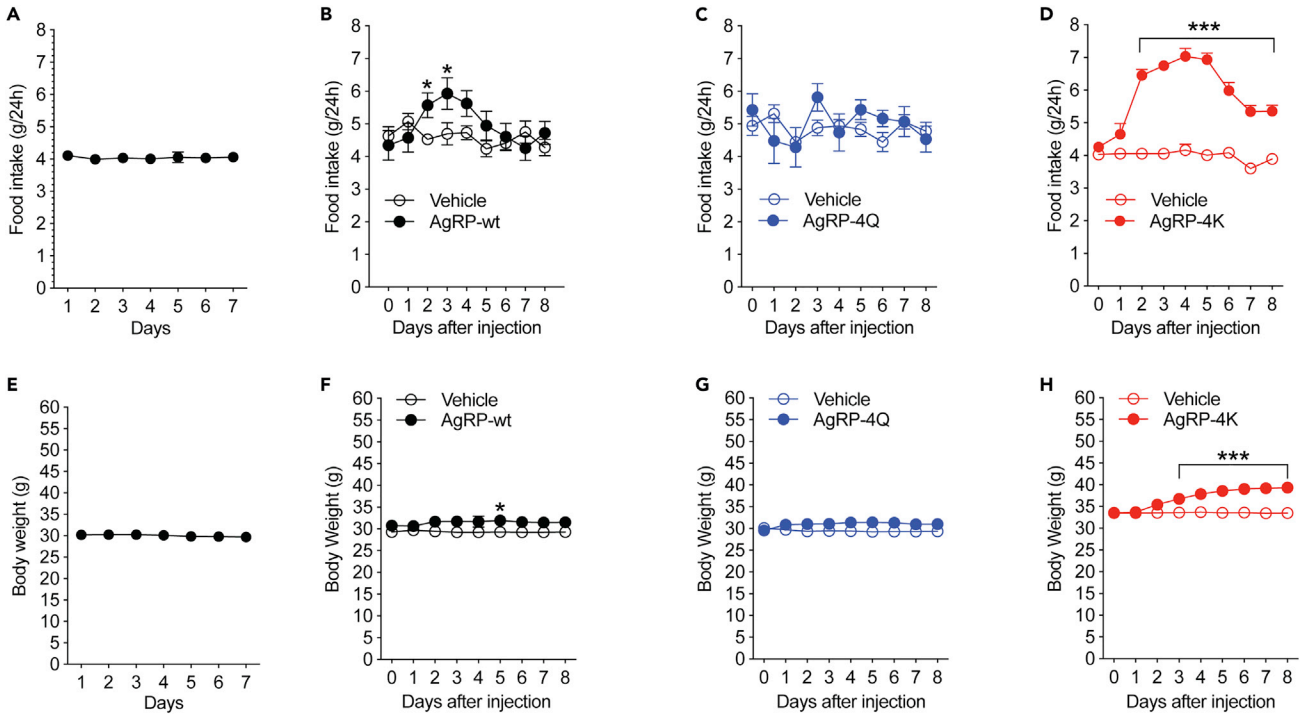

Figure 4. Effects of AgRP and Charge-Modified AgRP Variants on *Ad Libitum* Food Intake and Body Weight

Baseline levels of food intake (A) and body weight (E) were recorded daily for seven days, and then the AgRP peptides were injected ICV in the lateral ventricle (1 nmol in 1 μL of saline).

(B) The mature wild-type form of AgRP (AgRP-WT) significantly increased the amount of food that was consumed. The two-way repeated-measures ANOVA revealed a significant main effect of days ($F_{8,152}$ = 3.65, p = 0.0006) and a significant AgRP variant × days interaction ($F_{8,152}$ = 3.736, p = 0.0005) n = 10–11/group. The *post hoc* analysis showed that the increases in food consumption were statistically significant on the second and third days of AgRP administration. *p < 0.05, compared with mice that were injected with vehicle; ***p < 0.001, compared with vehicle group (*post hoc* test). n = 10–11/group.

(C) The mutant form with lower positive charges (AgRP-4Q) did not significantly alter *ad libitum* food consumption.

(D) The mutant form with higher positive charges (AgRP-4K) caused a significant and long-lasting increase in food intake, which peaked on the second day of injection. The two-way repeated-measures ANOVA revealed significant main effects of AgRP ($F_{1,25}$ = 143.2, p < 0.0001) and time course ($F_{8,200}$ = 25.65, p < 0.0001) and a significant AgRP × time course interaction ($F_{8,200}$ = 20.85, p < 0.0001). (F) AgRP-WT caused a transient significant increase in body weight on day 5 post-injection. (G) AgRP-4Q did not affect body weight. (H) AgRP-4K caused a significant increase in body weight that started on day 3 post-injection, which lasted through the testing period. The two-way repeated-measures ANOVA revealed significant main effects of AgRP ($F_{1,25}$ = 9.403, p < 0.01) and time course ($F_{8,200}$ = 127.5, p < 0.0001) and a significant AgRP × time course interaction ($F_{8,200}$ = 125.2, p < 0.0001). ***p < 0.001, compared with vehicle group (*post hoc* test). n = 13–14/group. Data are represented as mean ± SEM.

to be required for feeding responses that are induced by palatable food that recruits hedonic neural circuits (Denis et al., 2015).

The present study investigated the effects of AgRP and its interaction with heparan sulfate on food intake and metabolism using $AgRP_{(83-132)}$, the mature form of AgRP (AgRP-WT), and two charge-modified AgRP variants (AgRP-4K and AgRP-4Q) with either a higher or lower density of positively charged amino acids outside the ICK motif, resulting in either higher or lower affinity for heparan sulfate, respectively. Because the ICK motif mediates the AgRP interaction with MC3/4R, AgRP-WT, AgRP-4Q, and AgRP-4K all have identical receptor affinities and potency *in vitro* (Madonna et al., 2012).

We found that the ICV administration of AgRP enhanced both *ad libitum* food intake in the home cage and the motivation for food in an operant paradigm, which were correlated with the density of positive charges of the AgRP variants. The AgRP-induced increase in *ad libitum* food intake was abolished in AgRP-4Q (i.e., the AgRP variant that had the least positive charges that also exhibited deficient heparan sulfate binding) and more pronounced and protracted with AgRP-4K (i.e., the most positively charged AgRP variant that also exhibited the greatest affinity for heparan sulfate). However, a rapid but transient increase in operant responding for food was observed in mice that were treated with AgRP-4Q. The increase in operant responding for food was delayed in mice that were treated with AgRP-4K, but the increase was protracted

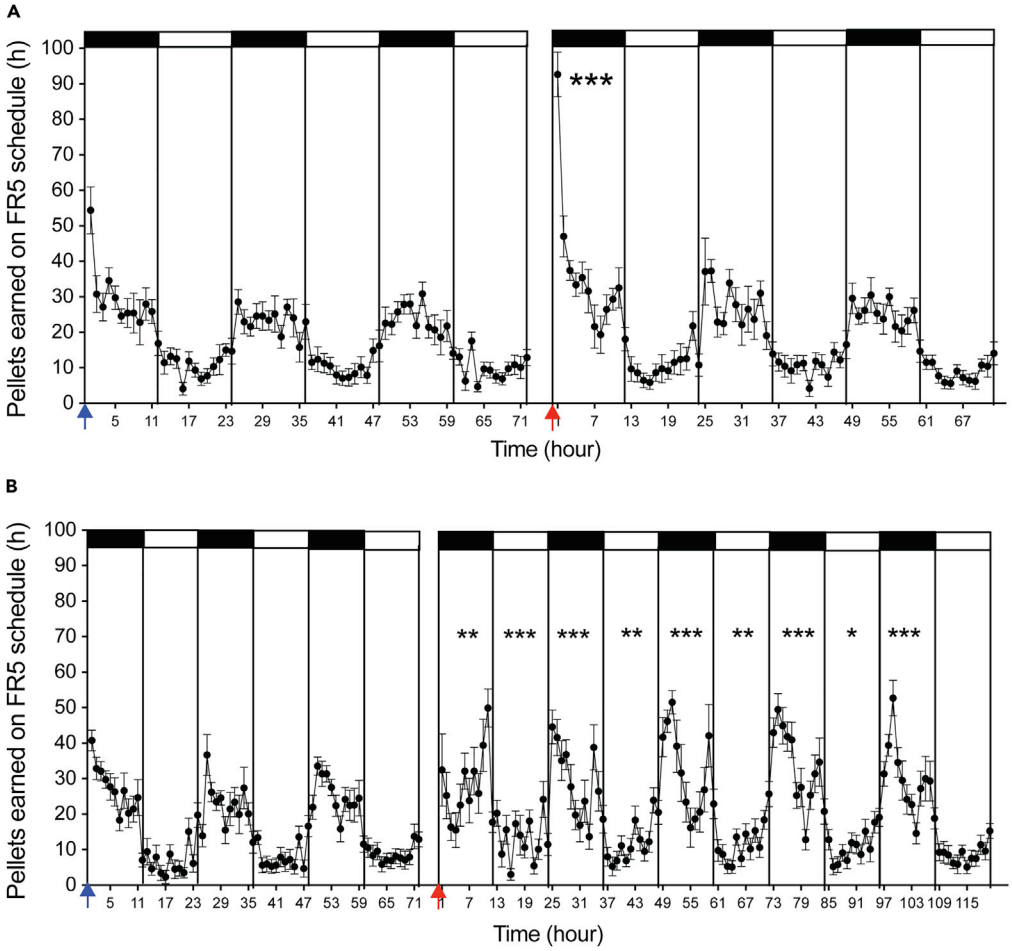

Figure 5. Effects of AgRP and Charge-Modified AgRP Variants on Operant Food Self-Administration

(A) AgRP-4Q significantly increased food self-administration during the dark phase on the first day of injection. This feeding-promoting effect of AgRP-4Q subsided rapidly in the following periods. The two-way repeated-measures ANOVA revealed significant main effects of AgRP variant ($F_{1,16} = 7.452$, $p = 0.015$) and time ($F_{7,112} = 183.4$, $p < 0.0001$) and a significant AgRP variant × time interaction ($F_{7,112} = 2.577$, $p = 0.017$). ***$p < 0.001$, relative to the level before AgRP injection.

(B) AgRP-4K induced a longer-lasting increase in food self-administration compared with AgRP-4Q. Data are represented as mean ± SEM.

and lasted for approximately four days. These results indicate that in addition to *ad libitum* food intake, AgRP increases the motivation for food, and both of these effects depended on its affinity for heparan sulfate. AgRP-WT and AgRP-4K also increased water intake, which was correlated with the increase in feeding and thus may reflect a general increase in consummatory behavior that was induced by the AgRP variants that exhibited higher positive charges and thus higher heparan sulfate binding affinity.

All of the AgRP variants that were tested herein reduced body temperature, suggesting a decrease in energy expenditure. The effect on body temperature of AgRP-4Q, the variant with a lower density of positive charges, had a faster onset and was less protracted. AgRP-WT decreased oxygen consumption (VO_2), indicating lower energy expenditure. A similar, although nonsignificant, trend toward a decrease in VO_2 was observed with AgRP-4K, the variant with higher positive charges, but not AgRP-4Q, the variant with lower positive charges.

AgRP-WT and AgRP-4K, but not AgRP-4Q, induced a protracted and significant increase in the RER at rest (during the light phase), indicating a reduction of fat oxidation and a shift toward carbohydrates as the predominant fuel source (Lusk, 1924; Marvyn et al., 2016; Schmidt-Nielsen, 1997; Speakman, 2013). In humans, overnight fasting is associated with high rates of fat oxidation (low RER), which is

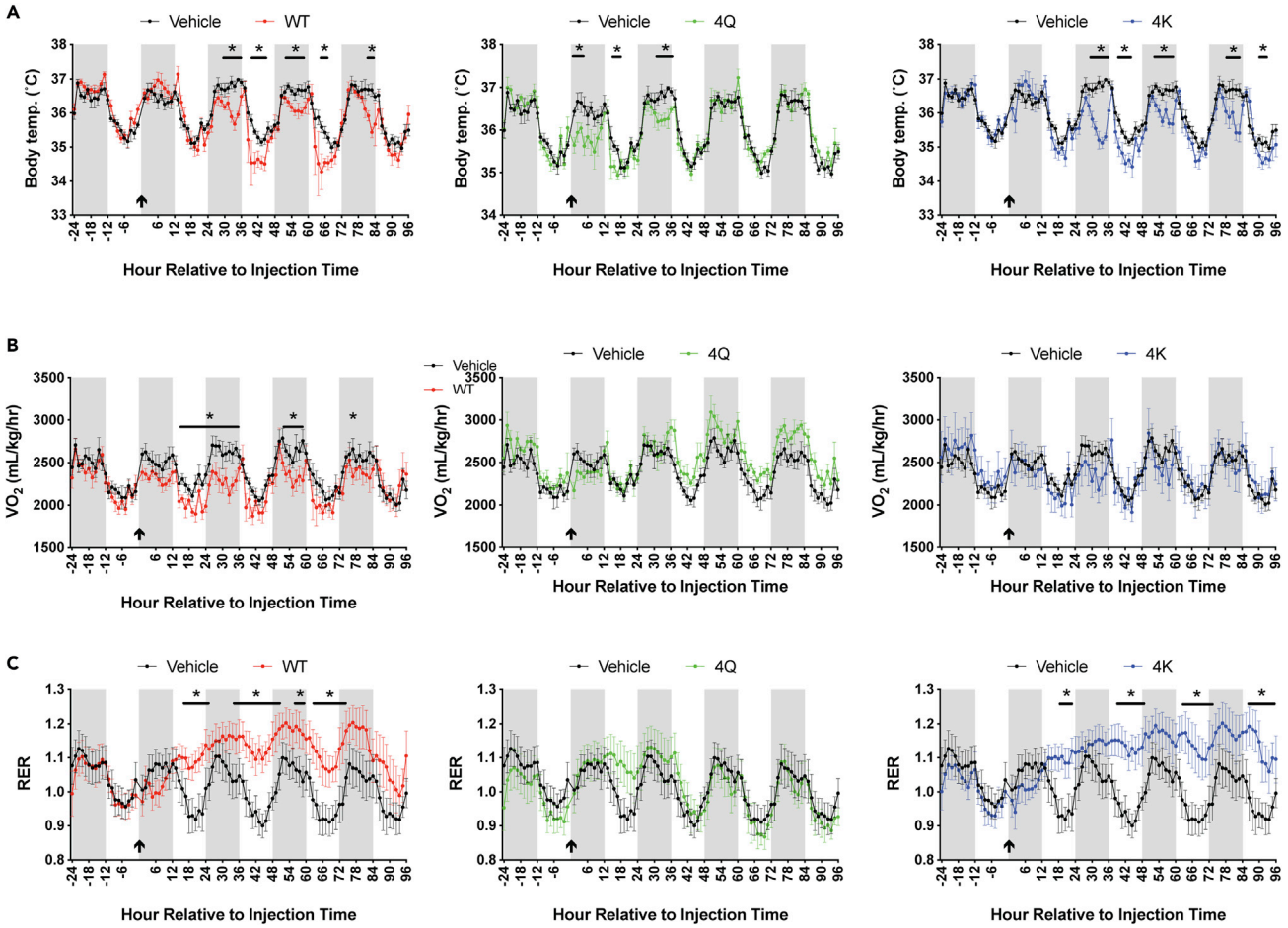

Figure 6. Effects of AgRP and Charge-Modified AgRP Variants on Energy Expenditure and Fuel Source

Energy expenditure was assessed by body temperature and VO_2 in the CLAMS.

(A) All three variants of AgRP—AgRP-WT (*left*), AgRP-4Q (*middle*), and AgRP-4K (*right*)—significantly decreased body temperature, suggesting that AgRP reduces energy expenditure. The effect of AgRP-4Q (*center*) had a faster onset and was less protracted than the effects of AgRP-WT (*left*) and AgRP-4K (*right*). Two-way repeated-measures ANOVA revealed significant AgRP variant × hours interactions for all three variants (AgRP-WT: $F_{99,990} = 2.225$, $p < 0.0001$; AgRP-4Q: $F_{99,856} = 1.754$, $p < 0.0001$; AgRP-4K: $F_{99,891} = 2.828$, $p < 0.0001$).

(B) VO_2 was significantly decreased by AgRP-WT, indicating that AgRP reduced energy expenditure.

(C) Effects of AgRP on the respiratory exchange rate (RER) in the CLAMS. AgRP-WT (*left*) and AgRP-4K (*right*) but not AgRP-4Q (*middle*) significantly increased the RER specifically during the light phase (AgRP-WT: F4.577,45.77 = 10.73, $p < 0.0001$; AgRP-4K: F6.708,60.37 = 24.91, $p < 0.0001$; AgRP-4Q: F3.734,37.20 = 11.38, $p < 0.05$), indicating that AgRP reduced fat oxidation and increased carbohydrate utilization as the predominant fuel source. *$p < 0.05$, compared with vehicle group (*post hoc* test). Data are represented as mean ± SEM.

blunted in individuals with a family history of type 2 diabetes (Ukropcova et al., 2007), reminiscent of the present results in AgRP-WT- and AgRP-4K-treated mice. Reduced fatty acid oxidation at rest promotes increased fat storage (Must et al., 1999), whereas exercise training can promote higher rates of fatty acid oxidation at rest as well as during acute exercise (van Loon et al., 1999). A high RER at rest (reduced fat oxidation and greater carbohydrate oxidation) in moderately overweight men has been linked to greater metabolic syndrome risk compared with a low RER (greater fat oxidation at rest; Rosenkilde et al., 2010). The increase in the RER in AgRP-WT- and AgRP-4K-treated mice appears to be consistent with findings of higher fat oxidation in mice with perinatal deletions of NPY/AgRP neurons (Cansell et al., 2012) and mice with the transgenic overexpression of heparanase, which selectively cleaves heparan sulfate chains (Karlsson-Lindahl et al., 2012).

The present results showed that AgRP increased both *ad libitum* food intake and operant responding for food, and these orexigenic effects of AgRP were accompanied by metabolic changes that were characterized by lower

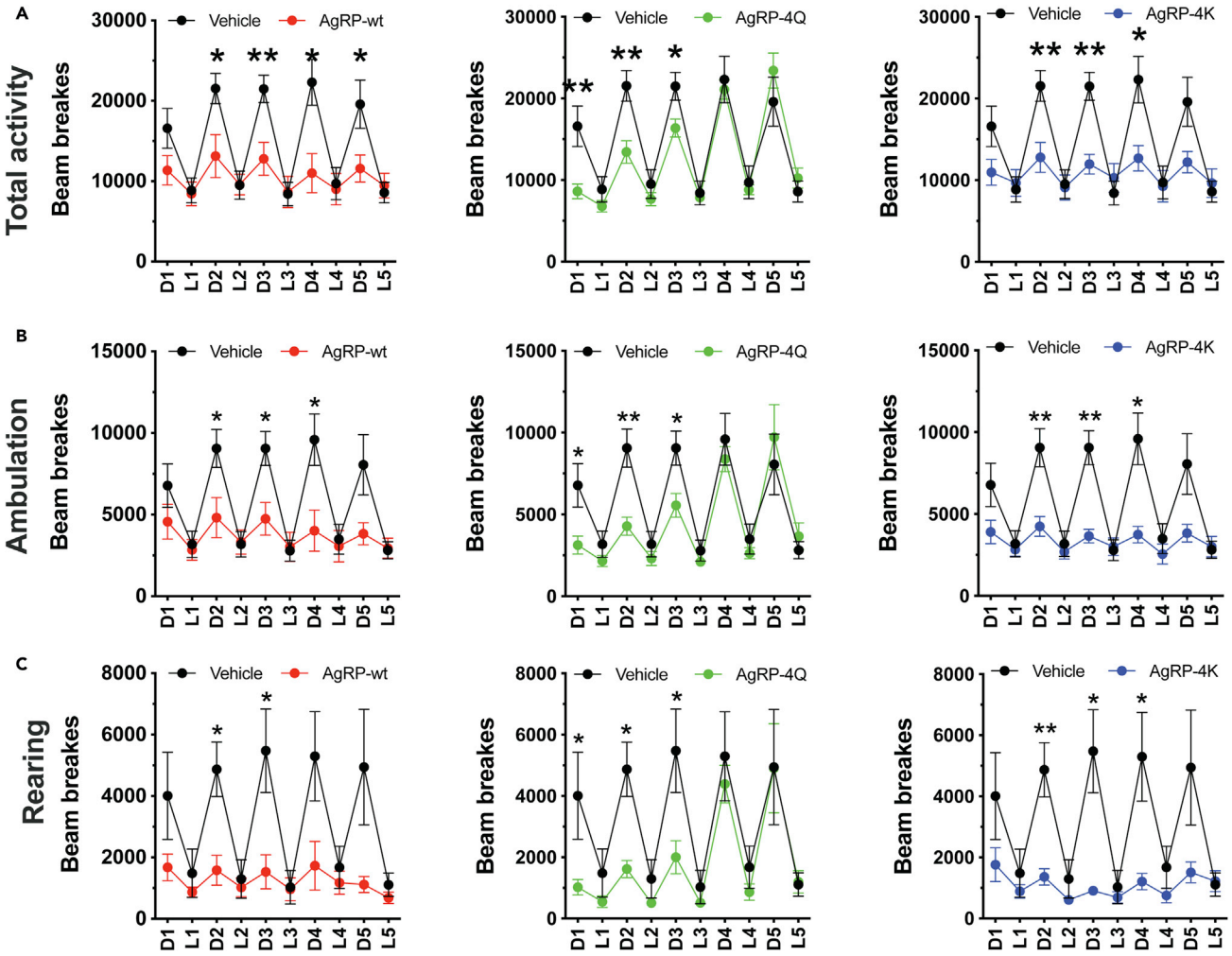

Figure 7. Effects of AgRP and Charge-Modified AgRP Variants on Activity

AgRP significantly decreased activity in mice, including total activity (A), ambulation (B), and rearing (vertical activity) (C) in the CLAMS. The effect of AgRP-4Q (*center*) had a faster onset and was less protracted than the effects of AgRP-WT (*left*) and AgRP-4K (*right*).

(A) All three variants of AgRP—AgRP-WT (*left*), AgRP-4Q (*middle*), and AgRP-4K (*right*)—reduced total activity, particularly during the dark phase. Total activity during the light phase was unaffected. The two-way repeated-measures ANOVA revealed a significant AgRP variant × hours interaction for all three variants (AgRP-WT: $F_{9,90} = 6.535$, $p < 0.0001$; AgRP-4Q: $F_{9,81} = 2.824$, $p = 0.0001$; AgRP-4K: $F_{9,90} = 8.464$, $p < 0.0001$).

(B) Ambulation. The two-way repeated-measures ANOVA revealed a significant AgRP variant × hours interaction for all three variants (AgRP-WT: $F_{9,90} = 4.824$, $p < 0.0001$; AgRP-4Q: $F_{9,81} = 2.844$, $p = 0.0058$; AgRP-4K: $F_{9,90} = 6.222$, $p < 0.0001$).

(C) Rearing. The two-way repeated-measures ANOVA revealed a significant AgRP variant × hours interaction for two of the variants (AgRP-WT: $F_{9,90} = 3.226$, $p = 0.0020$; AgRP-4K: $F_{9,90} = 3.767$, $p = 0.0005$). *$p < 0.05$, **$p < 0.01$, ***$p < 0.001$, significant difference between AgRP and vehicle groups. The data are presented in the form of a 12 h/12 h light/dark cycle. D, dark phase; L, light phase. *$p < 0.05$, **$p < 0.01$, compared with vehicle group (*post hoc* test). Data are represented as mean ± SEM.

energy expenditure and a reduction of fat utilization as the fuel source. These actions generally depended on the density of positively charged amino acids, indicating that the affinity of AgRP for heparan sulfate is a key determinant of both the orexigenic and metabolic effects of AgRP. The delayed and protracted kinetics of most actions of AgRP-WT and AgRP-4K, which can interact with heparan sulfate unlike AgRP-4Q, are consistent with a role for heparan sulfate proteoglycans in the extracellular matrix in controlling the diffusion of heparan/heparin-binding peptides that act as storage mechanisms (Kim et al., 2011; Reizes et al., 2001; Sarrazin et al., 2011). This function of heparan sulfate proteoglycans in the extracellular matrix results in the establishment of gradients of signaling peptides during development and has been proposed to act as a repository of growth factors that possibly results in their sequestration or localization in the proximity of receptors and prolongation of their action (Kim et al., 2011; Reizes et al., 2001; Sarrazin et al., 2011).

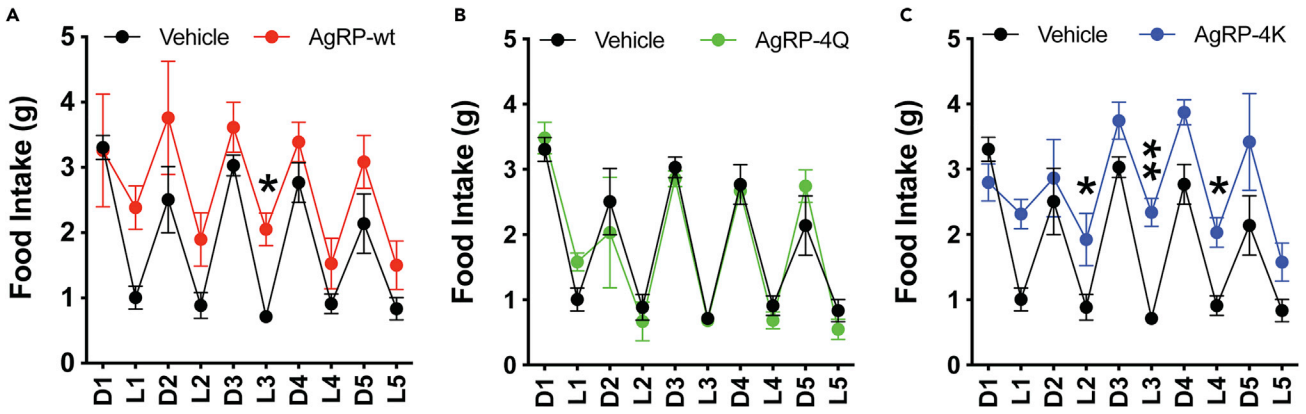

Figure 8. Effects of AgRP and Charge-Modified AgRP Variants on Food Intake in the CLAMS

Mice received AgRP-WT, AgRP-4Q, and AgRP-4K injections in the lateral ventricles, and food intake was monitored in the CLAMS for the following five days. AgRP-WT (A) and AgRP-4K (C) but not AgRP-4Q (B) increased food intake compared with the vehicle-treated group. All of the CLAMS experiments were performed under a 12 h/12 h light/dark cycle. D, dark phase; L, light phase. *p < 0.05, **p < 0.01, compared with vehicle group (*post hoc* test). Data are represented as mean ± SEM.

The differential effects of AgRP on feeding and various aspects of metabolic regulation that were observed in the present study may reflect complex anatomical relationships between NPY/AgRP neurons in the ARC and their energy-relevant connections (Betley et al., 2013; Sternson and Atasoy, 2014). Populations of NPY/AgRP neurons with segregated axonal projections that differentially innervate target brain regions have been observed with cell-type-specific neuron manipulations (Betley et al., 2013; Sternson and Atasoy, 2014). A low rate of ARC neuron collateralization has been reported in rats and mice (Betley et al., 2013; Chronwall, 1985; Sternson and Atasoy, 2014). The optogenetic activation of NPY/AgRP neurons has shown that different projections of NPY/AgRP neurons are involved in the long-term regulation of feeding behavior through POMC/CART neurons and the acute control of appetite through an interconnected forebrain circuit that includes the paraventricular nucleus of the hypothalamus, anterior bed nucleus of the stria terminalis, and lateral hypothalamus, among other regions that are involved in feeding behavior (Betley et al., 2013; Sternson and Atasoy, 2014). The regulation of different NPY/AgRP neuronal populations appears to be specific. For example, the responsiveness to ghrelin and food deprivation characterizes both intrahypothalamic and extrahypothalamic NPY/AgRP neuronal projection subpopulations. The leptin receptor is expressed in NPY/AgRP neurons that project outside of the hypothalamus but not in neurons that project within the hypothalamus (Betley et al., 2013; Sternson and Atasoy, 2014). These considerations suggest that distinct NPY/AgRP neuronal projections may subserve the regulation of energy metabolism and food intake and that the duration and intensity of AgRP's actions on food intake and metabolism are differentially affected by the positive charges of AgRP and its affinity for heparan sulfate.

Conclusions

The present results indicate that the orexigenic effects of AgRP are accompanied by complex metabolic changes that are characterized by lower energy expenditure, a reduction of fat oxidation, and a shift in substrate utilization

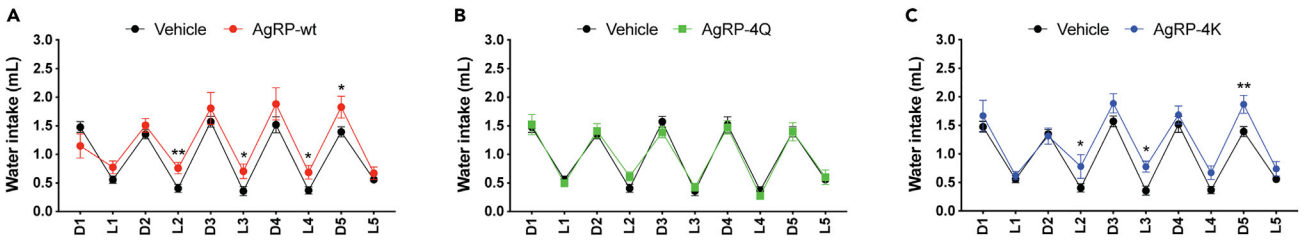

Figure 9. Effects of AgRP and Charge-Modified AgRP Variants on Water Intake in the CLAMS

AgRP-WT (A) and AgRP-4K (C) but not AgRP-4Q (B) increased water intake. The two-way repeated-measures ANOVA revealed significant main effects of AgRP-WT ($F_{1,18}$ = 4.499, p = 0.048) and AgRP-4K ($F_{1,18}$ = 6.265, p = 0.022). D, dark phase; L, light phase. *p < 0.05, **p < 0.01, compared with vehicle group (*post hoc* test). Data are represented as mean ± SEM.

toward carbohydrate oxidation. To investigate the effects of AgRP and its interaction with heparan sulfate on food intake and metabolism, we used the mature form of AgRP and two additional charge-modified AgRP variants with either a higher or a lower density of positively charged amino acids outside the receptor-binding motif, resulting in either an increase or a decrease in binding to heparan sulfate, respectively. The AgRP variants that were tested had identical MC3/4R receptor affinity and *in vitro* potency, but we observed significant differences between their orexigenic and metabolic responses *in vivo*. The *in vivo* potency and duration of action of AgRP largely depended on positively charged amino acids that mediate heparan sulfate binding independently of MC3/4R receptor binding. Overall, the present results support a role for AgRP and its interaction with heparan sulfate in the regulation of energy expenditure and metabolic balance between carbohydrate and lipid utilization.

Limitations of the Study

Despite convincing evidence that heparan sulfate proteoglycans are key modulators of the actions of AgRP, we cannot exclude the potential contribution of other complementary mechanisms for AgRP positive charges in potentiating and prolonging its orexigenic and metabolic effects. For instance, AgRP positive charge density may have effects at the receptor level, such as the stabilization of alternative active states of MC3Rs and MC4Rs, and may act as a biased agonist at MC4Rs on the regulation of Kir7.1 potassium channels (Ghamari-Langroudi et al., 2015) or on the recruitment of β-arrestins (Breit et al., 2006). Future studies will also investigate whether AgRP is also bound by other glycosaminoglycans, such as chondroitin sulfate.

ACKNOWLEDGMENTS

Supported by National Institutes of Health grants DK110403, AA021667, DA041750, DA043268, DA046170, DA046204, and DA048882. We are grateful to Dr. James C. Paulson (The Scripps Research Institute) for valuable discussions and encouragement. The authors thank Michael Arends for assistance with manuscript preparation and editing.

AUTHOR CONTRIBUTIONS

Conceptualization: P.P.S. and G.L.M. Methodology and investigation: J.C., V.C., T.K., Y.Y., I.H., A.W., R.M.B., V.R.C., and P.P.S. Data analysis: J.C., V.C., T.K., I.H., R.M.B., and V.R.C. Manuscript writing: J.C., V.C., T.K., P.P.S., and G.L.M. Review and editing: J.C., V.C., T.K., Y.Y., I.H., A.W., R.M.B., J.C.P., V.R.C., G.L.M., and P.P.S. Funding acquisition: P.P.S. and G.L.M.

DECLARATION OF INTERESTS

The authors declare no conflict of interest.

Received: July 23, 2019
Revised: September 21, 2019
Accepted: October 25, 2019
Published: December 20, 2019

REFERENCES

Andermann, M.L., and Lowell, B.B. (2017). Toward a wiring diagram understanding of appetite control. Neuron *95*, 757–778.

Aponte, Y., Atasoy, D., and Sternson, S.M. (2011). AGRP neurons are sufficient to orchestrate feeding behavior rapidly and without training. Nat. Neurosci. *14*, 351–355.

Betley, J.N., Cao, Z.F., Ritola, K.D., and Sternson, S.M. (2013). Parallel, redundant circuit organization for homeostatic control of feeding behavior. Cell *155*, 1337–1350.

Breit, A., Wolff, K., Kalwa, H., Jarry, H., Buch, T., and Gudermann, T. (2006). The natural inverse agonist agouti-related protein induces arrestin-mediated endocytosis of melanocortin-3 and -4 receptors. J. Biol. Chem. *281*, 37447–37456.

Butler, A.A., Kesterson, R.A., Khong, K., Cullen, M.J., Pelleymounter, M.A., Dekoning, J., Baetscher, M., and Cone, R.D. (2000). A unique metabolic syndrome causes obesity in the melanocortin-3 receptor-deficient mouse. Endocrinology *141*, 3518–3521.

Cansell, C., Denis, R.G., Joly-Amado, A., Castel, J., and Luquet, S. (2012). Arcuate AgRP neurons and the regulation of energy balance. Front. Endocrinol. (Lausanne) *3*, 169.

Chen, A.S., Marsh, D.J., Trumbauer, M.E., Frazier, E.G., Guan, X.M., Yu, H., Rosenblum, C.I., Vongs, A., Feng, Y., Cao, L., et al. (2000). Inactivation of the mouse melanocortin-3 receptor results in increased fat mass and reduced lean body mass. Nat. Genet. *26*, 97–102.

Chen, J., Repunte-Canonigo, V., Kawamura, T., Lefebvre, C., Shin, W., Howell, L.L., Hemby, S.E., Harvey, B.K., Califano, A., Morales, M., et al. (2013). Hypothalamic proteoglycan syndecan-3 is a novel cocaine addiction resilience factor. Nat. Commun. *4*, 1955.

Chronwall, B.M. (1985). Anatomy and physiology of the neuroendocrine arcuate nucleus. Peptides *6* (*Suppl 2*), 1–11.

Cone, R.D., Cowley, M.A., Butler, A.A., Fan, W., Marks, D.L., and Low, M.J. (2001). The arcuate nucleus as a conduit for diverse signals relevant to energy homeostasis. Int. J. Obes. Relat. Metab. Disord. *25* (*Suppl 5*), S63–S67.

Creemers, J.W., Pritchard, L.E., Gyte, A., Le Rouzic, P., Meulemans, S., Wardlaw, S.L., Zhu, X., Steiner, D.F., Davies, N., Armstrong, D., et al.

(2006). Agouti-related protein is posttranslationally cleaved by proprotein convertase 1 to generate agouti-related protein (AGRP)83-132: interaction between AGRP83-132 and melanocortin receptors cannot be influenced by syndecan-3. Endocrinology *147*, 1621–1631.

Deng, J., Yuan, F., Guo, Y., Xiao, Y., Niu, Y., Deng, Y., Han, X., Guan, Y., Chen, S., and Guo, F. (2017). Deletion of ATF4 in AgRP neurons promotes fat loss mainly via increasing energy expenditure. Diabetes *66*, 640–650.

Denis, R.G., Joly-Amado, A., Webber, E., Langlet, F., Schaeffer, M., Padilla, S.L., Cansell, C., Dehouck, B., Castel, J., Delbes, A.S., et al. (2015). Palatability can drive feeding independent of AgRP neurons. Cell Metab. *22*, 646–657.

Dodd, G.T., and Tiganis, T. (2017). Insulin action in the brain: roles in energy and glucose homeostasis. J. Neuroendocrinol. *29*, https://doi.org/10.1111/jne.12513.

Ehtesham, S., Qasim, A., and Meyre, D. (2019). Loss-of-function mutations in the melanocortin-3 receptor gene confer risk for human obesity: a systematic review and meta-analysis. Obes. Rev. *20*, 1085–1092.

Ghamari-Langroudi, M., Digby, G.J., Sebag, J.A., Millhauser, G.L., Palomino, R., Matthews, R., Gillyard, T., Panaro, B.L., Tough, I.R., Cox, H.M., et al. (2015). G-protein-independent coupling of MC4R to Kir7.1 in hypothalamic neurons. Nature *520*, 94–98.

Goodfellow, V.S., and Saunders, J. (2003). The melanocortin system and its role in obesity and cachexia. Curr. Top. Med. Chem. *3*, 855–883.

Kalra, S.P., Dube, M.G., Pu, S., Xu, B., Horvath, T.L., and Kalra, P.S. (1999). Interacting appetite-regulating pathways in the hypothalamic regulation of body weight. Endocr. Rev. *20*, 68–100.

Karlsson-Lindahl, L., Schmidt, L., Haage, D., Hansson, C., Taube, M., Egeciouglu, E., Tan, Y.X., Admyre, T., Jansson, J.O., Vlodavsky, I., et al. (2012). Heparanase affects food intake and regulates energy balance in mice. PLoS One *7*, e34313.

Kim, S.H., Turnbull, J., and Guimond, S. (2011). Extracellular matrix and cell signalling: the dynamic cooperation of integrin, proteoglycan and growth factor receptor. J. Endocrinol. *209*, 139–151.

Konner, A.C., Janoschek, R., Plum, L., Jordan, S.D., Rother, E., Ma, X., Xu, C., Enriori, P., Hampel, B., Barsh, G.S., et al. (2007). Insulin action in AgRP-expressing neurons is required for suppression of hepatic glucose production. Cell Metab. *5*, 438–449.

Krashes, M.J., Koda, S., Ye, C., Rogan, S.C., Adams, A.C., Cusher, D.S., Maratos-Flier, E., Roth, B.L., and Lowell, B.B. (2011). Rapid, reversible activation of AgRP neurons drives feeding behavior in mice. J. Clin. Invest. *121*, 1424–1428.

Krashes, M.J., Shah, B.P., Koda, S., and Lowell, B.B. (2013). Rapid versus delayed stimulation of feeding by the endogenously released AgRP neuron mediators GABA, NPY, and AgRP. Cell Metab. *18*, 588–595.

Lede, V., Franke, C., Meusel, A., Teupser, D., Ricken, A., Thiery, J., Schiller, J., Huster, D., Schoneberg, T., and Schulz, A. (2016). Severe atherosclerosis and hypercholesterolemia in mice lacking both the melanocortin type 4 receptor and low density lipoprotein receptor. PLoS One *11*, e0167888.

Loh, K., Herzog, H., and Shi, Y.C. (2015). Regulation of energy homeostasis by the NPY system. Trends Endocrinol. Metab. *26*, 125–135.

Lusk, G. (1924). Animal calorimetry: twenty-fourth paper. Analysis of the oxidation of mixtures of carbohydrate and fat. J. Biol. Chem. *59*, 41–42.

Madonna, M.E., Schurdak, J., Yang, Y.K., Benoit, S., and Millhauser, G.L. (2012). Agouti-related protein segments outside of the receptor binding core are required for enhanced short- and long-term feeding stimulation. ACS Chem. Biol. *7*, 395–402.

Marvyn, P.M., Bradley, R.M., Mardian, E.B., Marks, K.A., and Duncan, R.E. (2016). Data on oxygen consumption rate, respiratory exchange ratio, and movement in C57BL/6J female mice on the third day of consuming a high-fat diet. Data Brief *7*, 472–475.

McNulty, J.C., Thompson, D.A., Bolin, K.A., Wilken, J., Barsh, G.S., and Millhauser, G.L. (2001). High-resolution NMR structure of the chemically-synthesized melanocortin receptor binding domain AGRP(87-132) of the agouti-related protein. Biochemistry *40*, 15520–15527.

Must, A., Spadano, J., Coakley, E.H., Field, A.E., Colditz, G., and Dietz, W.H. (1999). The disease burden associated with overweight and obesity. JAMA *282*, 1523–1529.

Nuutinen, S., Ailanen, L., Savontaus, E., and Rinne, P. (2018). Melanocortin overexpression limits diet-induced inflammation and atherosclerosis in LDLR(-/-) mice. J. Endocrinol. *236*, 111–123.

Obici, S., Zhang, B.B., Karkanias, G., and Rossetti, L. (2002). Hypothalamic insulin signaling is required for inhibition of glucose production. Nat. Med. *8*, 1376–1382.

Palomino, R., Lee, H.W., and Millhauser, G.L. (2017). The agouti-related peptide binds heparan sulfate through segments critical for its orexigenic effects. J. Biol. Chem. *292*, 7651–7661.

Pocai, A., Lam, T.K., Gutierrez-Juarez, R., Obici, S., Schwartz, G.J., Bryan, J., Aguilar-Bryan, L., and Rossetti, L. (2005). Hypothalamic K(ATP) channels control hepatic glucose production. Nature *434*, 1026–1031.

Reizes, O., Lincecum, J., Wang, Z., Goldberger, O., Huang, L., Kaksonen, M., Ahima, R., Hinkes, M.T., Barsh, G.S., Rauvala, H., et al. (2001). Transgenic expression of syndecan-1 uncovers a physiological control of feeding behavior by syndecan-3. Cell *106*, 105–116.

Rosenkilde, M., Nordby, P., Nielsen, L.B., Stallknecht, B.M., and Helge, J.W. (2010). Fat oxidation at rest predicts peak fat oxidation during exercise and metabolic phenotype in overweight men. Int. J. Obes. (Lond.) *34*, 871–877.

Sarrazin, S., Lamanna, W.C., and Esko, J.D. (2011). Heparan sulfate proteoglycans. Cold Spring Harb. Perspect. Biol. *3*, a004952.

Schioth, H.B., Chhajlani, V., Muceniece, R., Klusa, V., and Wikberg, J.E. (1996). Major pharmacological distinction of the ACTH receptor from other melanocortin receptors. Life Sci. *59*, 797–801.

Schmidt-Nielsen, K. (1997). Animal Physiology (Cambridge University Press).

Speakman, J.R. (2013). Measuring energy metabolism in the mouse - theoretical, practical, and analytical considerations. Front. Physiol. *4*, 34.

Steculorum, S.M., Ruud, J., Karakasilioti, I., Backes, H., Engstrom Ruud, L., Timper, K., Hess, M.E., Tsaousidou, E., Mauer, J., Vogt, M.C., et al. (2016). AgRP neurons control systemic insulin sensitivity via myostatin expression in brown adipose tissue. Cell *165*, 125–138.

Sternson, S.M., and Atasoy, D. (2014). Agouti-related protein neuron circuits that regulate appetite. Neuroendocrinology *100*, 95–102.

Ukropcova, B., Sereda, O., de Jonge, L., Bogacka, I., Nguyen, T., Xie, H., Bray, G.A., and Smith, S.R. (2007). Family history of diabetes links impaired substrate switching and reduced mitochondrial content in skeletal muscle. Diabetes *56*, 720–727.

van der Klaauw, A.A. (2018). Neuropeptides in obesity and metabolic disease. Clin. Chem. *64*, 173–182.

van Loon, L.J., Jeukendrup, A.E., Saris, W.H., and Wagenmakers, A.J. (1999). Effect of training status on fuel selection during submaximal exercise with glucose ingestion. J. Appl. Physiol. (1985) *87*, 1413–1420.

Williams, G., Bing, C., Cai, X.J., Harrold, J.A., King, P.J., and Liu, X.H. (2001). The hypothalamus and the control of energy homeostasis: different circuits, different purposes. Physiol. Behav. *74*, 683–701.